In: *The Cognitive Neurosciences*, Third Edition, M. S. Gazzaniga (ed), MIT Press, 2004, pp. 511-524.

Motor Learning and Memory for Reaching and Pointing

REZA SHADMEHR AND STEVEN P. WISE

REZA SHADMEHR Department of Biomedical Engineering, Johns Hopkins School of Medicine, 419 Traylor Building, 720 Rutland Avenue, Baltimore, Maryland

STEVEN P. WISE Laboratory of Systems Neuroscience, National Institute of Mental Health, Building 49, Room B1EE17, MSC 4401, 49 Convent Drive, Bethesda, Maryland

Abstract: 199 words

6,771 words in main body of text

7 figures and legends.

ABSTRACT To control reaching and pointing movements, the primate motor system draws upon vision, audition and other sensory modalities to estimate hand and target locations. We argue that the motor system represents these variables in visual coordinates, relative to the fixation point. According to a computational theory presented here, neural networks in the parietal cortex align information about muscle lengths and joint angles with an estimate of hand location relative to the fixation point. Related networks in parietal and frontal cortex, together with the cerebellum and basal ganglia, align the desired hand displacements—also in visual coordinates—with the joint rotations and forces needed to reach the target. The motor system updates these estimates when the eye changes orientation and whenever the hand or target changes location. Each network learns an internal model (IM) of the relationships among these sensorimotor variables, and, in so doing, computes coordinate transforms and predictions about the limb's future state. In motor learning, IMs adapt to distortions in visual feedback and altered limb dynamics. This process begins with adaptation of existing IMs and results—after extensive practice—in the formation of new ones: the motor system has acquired a new skill.

This chapter develops a computational theory of reaching and pointing in primates, one that owes much to previous ideas (Bullock and Grossberg, 1988; Cisek, Grossberg, and Bullock, 1998; Burnod et al., 1999; Andersen and Buneo, 2002).

Visually guided reaching in theory

We begin with a heuristic exercise in "virtual robotics." Many robotic arms have a gripper, which serves as the *end effector*. End effectors include anything that biological or robotic arms control: hands, robotic grippers, sticks, laser pointers, and cursors controlled by a computer mouse. Robot engineers have devised many solutions to the problem of programming a robotic arm to move its end effector to a target. Some begin by determining the location of the target with respect to the location of the gripper. If the robot has a video camera, our imaginary engineer can use its signal to determine the location of both the end effector and the target (

Figure 1A). The end-effector (*ee*) and target (*t*) locations, x_{ee} and x_t, respectively, define vectors in "camera-centered" coordinates, *i.e.*, a coordinate system that indicates the pixels occupied by both objects relative to some origin. The difference between these two vectors results in a third vector, x_{dv}, called the *difference vector*. It represents a high-order plan for movement.

Although our engineer has no choice but to use the camera to detect target location, he or she might use the lengths of each link of the robot's arm, together the angle (θ) of each joint, to compute an estimate of the gripper's location. This computation is called *forward kinematics*[1]. The engineer could write a program to ensure that the gripper's location as estimated through forward kinematics always matches the location recorded by the camera. This program could be said to *align* inputs from the camera and joint-angle sensors, and for the motor system, the analogous computation can be said to align an estimate of end-effector location in *visual and proprioceptive coordinates.*

To align the robot's "proprioception" with its "vision", the engineer might use two neural networks with feed-forward connections. One network would *map* proprioception to vision (*i.e.*, it would compute forward kinematics, as described above) and another network would map vision to proprioception (called *inverse kinematics*). However, a better approach is to use a single neural network, one that finds the best alignment between the two sensory variables through feedback between the network's hidden layer and all of its input and output layers. This kind of network dynamics cleans up noise and can compute arbitrary transformations (Deneve, Latham, and Pouget, 2001). The neural network depicted in

Figure 1B has this architecture: it finds an alignment between an arm configuration $\hat{\theta}$ and an estimate of gripper location $\hat{x}_{ee}$ (network 1 of

Figure 2) [2]. We denote the network and its transformational mapping with the symbol $\hat{\theta} \leftrightarrow \hat{x}_{ee}$ and call it the *location map*. When this expression is viewed from left to right, this network appears to compute forward kinematics: $f(\hat{\theta}) = \hat{x}_{ee}$. Alternatively, viewed from right to left, it computes inverse kinematics: $f^{-1}(\hat{x}_{ee}) = \hat{\theta}$, *i.e.,* the network finds one of the several arm configurations for a given end-effector location. In a sense, the network underlying the location map does not explicitly compute either forward- or inverse kinematics, but rather completes the "pattern" of whatever information it lacks, given the information it receives. Forward- and inverse kinematics emerge as the product of this *pattern-completion network*, and its computations correspond to an *internal model* (IM) of a relationship among the aligned variables.

The next step in planning a reaching movement involves comparing $\hat{x}_{ee}$ with $\hat{x}_t$ and computing a difference vector $x_{dv} = \hat{x}_t - \hat{x}_{ee}$. In the present model, another neural network with bidirectional connections performs this subtraction (network 3 in Figure 2). It is important to note, however, that while the vector x_{dv} always points from the robot's gripper to the target, its coordinates system remain camera-centered.

Once this system has computed a difference vector in camera-centered coordinates, it can use the results of that computation to move the robot's arm. Thus, the final step in planning a movement involves associating the difference vector x_{dv} with joint rotations $\Delta\hat{\theta}$. Unlike network 1, which aligns the robot's "vision" and "proprioception" for *locations,* network 4 aligns information regarding end-effector *displacements*. Thus, we call network 4 a *displacement map*. Later, we will argue that the distinction between location and displacement maps helps in understanding motor learning. For the present, note that—like the location map—the displacement map appears to compute either forward- or inverse kinematics. Viewed from left to right, it performs the key inverse-kinematics computation of traditional motor-control theory. From right to left, it aligns movement commands with predicted end-effector displacements.

For the desired displacement illustrated in Figure 1A, the alignment between a gripper displacement x_{dv} and joint rotations $\Delta\hat{\theta}$ must depend on $\hat{\theta}$, which reflects the current arm configuration. The following symbolism denotes this dependence: $x_{dv} \overset{\hat{\theta}}{\longleftrightarrow} \Delta\hat{\theta}$. As movement begins, the sensor readings will change. The joint- and camera sensors update their estimate of arm configuration, which, in turn, leads to a new x_{dv} until $x_{dv} \to 0$. Reaching involves an additional map, depicted as network 5 in Figure 2, which involves the alignment of joint rotations and force commands. We denote this mapping as $\Delta\hat{\theta} \overset{\hat{\theta}}{\longleftrightarrow} \hat{f}$ and call it a *dynamics map*.

Learning location and displacement maps

One of the most important features of our imaginary robot is its adaptive element: the program that aligns the gripper location that the camera records with that based on joint-angle transducers. If the alignment algorithm did not adapt, the robot would have trouble if the camera's optics or orientation changed.

Primates can, however, adapt to radical distortions in visual inputs. In one study, a monkey was fitted with dove prisms, which invert images along the left–right plane (Sugita, 1996). For the first few weeks of continuous prism-wearing, the monkeys could barely move, but after four weeks their movements improved markedly. Each day the monkeys attempted to reached to a sequence of targets. In 1–2 months, the monkeys began to reach accurately to the targets, and similar results have been obtained by Sekiyama, Miyauchi, Imaruoka, Egusa, and Tashiro (2000) in humans.

If the motor system uses location and displacement maps that align proprioceptive and visual signals (networks 1 and 4 of

Figure 2), then these maps must have changed during prism adaptation. What happened to the information that was contained in the maps for normal vision? After two months, the prisms were removed and, for a day or so, the monkeys again had trouble moving. They reached to the right when targets appeared to the left, a result of adaptation called an *aftereffect*. However, unlike the many weeks that it took the monkeys to adapt to the dove prisms, the aftereffects "washed out" by the third day. The slowness of initial adaptation and the rapidity of washout suggest that the prisms slowly changed the network in a way that accommodated the new alignment without losing the previous one. In the context of

Figure 2, we propose that some neural network gained an additional attractor state for its activity and this attractor caused networks 1 and 4 to compute a different transform. Many neural networks have dynamics that converge when their internal states fall into an attractor, which corresponds to something like a "preferred-activity state" of a network. According to this model, as a new attractor forms, the system gains a new capability, corresponding to a new motor skill. The networks' weight matrices have, at this point, been trained to solve both problems. According to this idea, some contextual input biases the networks collectively toward one or the other skill.

Adaptation to other kinds of prisms occurs much faster than for dove prisms. Typically, these prisms shift light by 5°–25°, rather than inverting the visual field. Participants adapt to such prisms in 5–10 trials, suggesting a shift in existing attractors, rather than the formation of new ones (Martin, Keating, Goodkin, Bastian, and Thach, 1996b). Removal of the prisms requires the same number of de-adaptation trials as the original adaptation. For this reason, adaptation with these prism glasses appears to result in the motor system regaining a former level of performance by shifting existing attractors. In contrast, perhaps skill acquisition leads to new capabilities by generating new attractors (Hallett, Pascual-Leone, and Topka, 1996).

The discussion to this point might lead to the conclusion that dove prisms induce new skills, but wedge prisms do not. However, with extensive experience, people can learn the "wedge-prism" skill, as well. After several weeks of practice, experienced prism-wearers eventually develop the ability to put on and remove the wedge prisms on demand with minimal adaptation times and aftereffects (Martin, Keating, Goodkin, Bastian, and Thach, 1996b). Effectively, their motor system learns to switch between alignments appropriate for the prism and those appropriate for normal vision based on a context: the wearing or freedom from prisms.

Our imaginary robot and its control networks can help explain prism adaptation. Imagine that a prism shifts the path of light so that, from the point-of-view of the camera, the visual world appears displaced to the left. Therefore, in

Figure 3A a target activates pixels on the camera to the left of the pixels that "should be" activated. The black ring indicates the viewed target location, as distorted by the prisms; the dotted circle shows the target's actual location, often called "real" space. Before the prism appeared on the scene, the control system had adaptively aligned the location map $\hat{\theta} \leftrightarrow \hat{x}_{ee}$ and the displacement map $x_{dv} \overset{\hat{\theta}}{\longleftrightarrow} \Delta\hat{\theta}$ in "visual" and "proprioceptive" coordinates.

Now assume that the camera cannot "see" the arm and so the system must estimate its location $\hat{x}_{ee}$ in camera-centered coordinates from "proprioception." Perhaps light must be conserved so that the camera only senses the light from a small light-emitting diode on the target and the room lights only flash on briefly at the end of the gripper's movement. The camera tells the central controller that the target is at x_t and the system computes a difference vector x_{dv} based on information from the joint-angle sensors in the robot's arm, as converted into camera-centered coordinates $\hat{\theta} \leftrightarrow \hat{x}_{ee}$, $x_{dv} = \hat{x}_t - \hat{x}_{ee}$.

Figure 3A illustrates this difference vector—in camera-centered coordinates—beneath the drawing of the robot. Using the displacement map $x_{dv} \overset{\hat{\theta}}{\longleftrightarrow} \Delta\hat{\theta}$, the controller computes a joint-rotation vector. This vector flexes the robot's "shoulder" (increasing θ_1) and extends its "elbow" (decreasing θ_2), bringing the arm in to the location indicated by the gray arm in

Figure 3B. After the movement ends, the camera records the gripper at the location shown by the black arm. The gripper missed the target to the left.

Note that the prism induced two kinds of errors. First, for the displacement map (network 4 in

Figure 2), the desired difference vector produced joint rotations that moved the gripper too far to the left. Second, for the location map (network 1 in

Figure 2), the camera recorded the gripper's location further to the left than it "should have been", according to the robot's joint angles. Therefore, in planning the next movement, the robotic controller should reduce the amount of flexion for the "shoulder" computed by the displacement map, as well as adaptively realign the location map. The controller requires visual feedback for such recalibrations, which changes its IMs. After these two IMs—the displacement and location maps—adapt, the robot can again direct its gripper to the target without visual feedback: *i.e.,* it regains its former level of performance.

Figure 3C shows the gripper's actual location in gray and the dotted line shows its estimated location in camera-centered coordinates from "proprioception." The system estimates the gripper's location to the left of its location in "real" space, but the system can compute a difference vector x_{dv} and map it to appropriate joint rotations. After adaptation to the prism, the displacement map estimates that target acquisition requires a smaller flexion in the "shoulder" angle along with a larger "elbow" extension. When the robot performs these joint rotations, the gripper moves to the gray location in

Figure 3D and the camera records it at the black location. In both "real" and camera-centered coordinates, the gripper reaches the target. After adaptation, targets at the illustrated location (away and to the left) map to joint rotations generating movements straight ahead (where the target actually is). Targets that appear straight ahead, induce joint rotations that move the gripper away and to the right.

Figure 3E illustrates what happens when we remove the prism and require the robot to make another reaching movement from the same starting location. The camera senses the target position at x_t, which is now its actual location, straight ahead. However, when the robot's controller computes x_{dv} and maps it to joint rotations, the system now estimates that to move the gripper to a target appearing straight ahead, it needs to extend the elbow and flex the shoulder according to the mappings learned when the prisms distorted the camera's input: away and to the right. This mapping causes the gripper to miss the target to the right: the *negative aftereffect* of adaptation.

The computations elaborated in our thought design have a number of interesting consequences, many of which have been tested in psychophysical experiments (Harris, 1965). For example, after participants in those experiments adapt to prisms, when they close their eyes and try to point straight ahead, they show aftereffects. These aftereffects arise because the imagined target $\hat{x}_t$ is the same as before the adaptation trials, but displacement map $x_{dv} \xleftarrow{\hat{\theta}} \Delta\hat{\theta}$ has changed. Further, when participants prism-adapt for reaching to a spatial auditory stimulus, and later remove the prisms, their movements to visual targets show aftereffects for the same reason. Finally, if participants prism-adapt with one hand, they show misreaching when they try to reach to that hand with their other hand. This aftereffect results from the change in $\hat{\theta} \leftrightarrow \hat{x}_{ee}$, the location map. The present model of prism adaptation resembles a previous three-factor model of prism adaptation (Welch, Choe, and Heinrich, 1974). It differs, however, in the present emphasis on extrinsic, vision-based coordinates for representing the target, end effector, and difference vector, as opposed to the body-centered coordinate frame assumed by that earlier model.

Updating the maps using efference copy

In the imaginary robot described so far, the camera never moves. Eyes are not like that, of course, and because the kinematic computations for reaching involve vision-based coordinates, eye movements pose a fundamental problem. Imagine that the target in

Figure 1A fell outside the camera's field of view. The robotic system described so far would be "lost". Without a target activating some pixels in the camera's field of view, the controller could not compute a difference vector and could not move the gripper to the target. To alleviate this problem, the engineer might place the camera on a swivel that reorients the camera so that it covers more territory. This benefit, however, comes at a cost: the location of the target in "real" space is no longer a simple function of which camera pixels the target activates. The controller now has to keep track of the camera's orientation.

To illustrate these points, imagine someone reading this book at a coffee shop. As that person reads, he or she reaches to the left for a note pad, as illustrated in Figure 4 (top, left). Because the person continues to orient gaze toward the book, the notepad $\hat{x}_t$ lies in his or her peripheral field of view. Now imagine that someone approaches that person from the right as reaching begins. Both the reader's head and eyes orient toward the right, but reaching remains accurate. Note that the reader did not look at the target initially and looked even further away from it when the other person approached.

When the reader's eyes and head moved, the location of the end effector and target changed in *retinotopic* coordinates, *i.e.,* the part of the retina on which the image of the target and end effector fell.

Although, eye movements resulted in a change in the location of $\hat{x}_t$ and x_{ee} in these retinotopic coordinates, the difference vector x_{dv} should have remained the same. According to the present model, changes in the orientation of the retina result in a re-calculation of the difference vector because of the changes in the retinotopic location of the target and end effector. We call the coordinate frame that is based on the eye's orientation, but independent of the visual field, *fixation-centered*, as opposed to *retinotopic*.

This fixation-centered frame corresponds to the camera-centered coordinates discussed for the imaginary robot but takes into account changes in the camera's orientation. A fixation-centered coordinate frame has two advantages over a retinotopic frame: fixation-centered coordinates can describe the location of the target and gripper beyond the retina's field of view and it can do so in three dimensions. The same "gain-field" mechanisms that have been invoked to compute target location in head- or body centered coordinates (Andersen, Bracewell, Barash, Gnadt, and Fogassi, 1990; Bremmer, Distler, and Hoffmann, 1997; Salinas and Abbott, 2001; Andersen and Buneo, 2002) can also be used to compute target- and end-effector location in fixation-centered coordinates as the eye's orientation changes. Gain-field networks essentially combine information about target location in retinotopic coordinates with information about the orientation of the eye to produce multiplicative computations that yield locations in some other coordinate frame. In the present model, these computations yield locations with respect to the fixation point.

Accordingly, the basic model sketched in

Figure 2 needs two augmentations: predictive *remapping* and the use of *efference copy.* First, reorientation of the retina, through eye movements, requires the control system to update the kinematic maps to reflect the changes in target- and end-effector locations relative to the fixation-point. Movements of the hand and the target also lead to updating. For posterior parietal cortex, there is neurophysiological evidence that the remembered location of a visual target, $\hat{x}_t$, is updated in fixation-centered coordinates as the eyes move (Duhamel, Colby, and Goldberg, 1992). Neurons in the lateral intraparietal area discharge after a saccade brings a stimulus into the cell's activity field, as well as when a saccade brings the location of a vanished stimulus into the cell's field (Figure 4B, bottom). Thus, it seems reasonable that as the eyes or the head moves, the motor system remaps both the representation of $\hat{x}_t$ and $\hat{x}_{ee}$ in fixation-centered coordinates. If a movement is to be made with the hand, motion of the eye and head produce an updating of x_{dv}.

Return to our example of reaching for a notepad while reading a book. Imagine that a breeze blows the notepad to the left as reaching begins (Figure 4). The updating mechanism ensures that the end

effector reaches the target: reaching movement terminates when the difference vector reaches zero. The motor system thus acts as an "autopilot", guiding the end effector to the target, and the posterior parietal cortex also has been implicated in this computation (Desmurget, Pelisson, Rossetti, and Prablanc, 1998; Desmurget et al., 1999; Grea et al., 2002).

This remapping must rely in large part on a copy of motor commands sent to oculomotor and skeletomotor systems, known as *efference copy*. The finding that remapping occurs predictively, *i.e.*, in advance of a saccadic eye movement (Duhamel et al., 1992), suggests an efference-copy based mechanism, and direct evidence for this idea has recently been reported for eye movements (Sommer and Wurtz, 2002). Thus, in predictive updating, the kinematic IMs depicted in

Figure 2 not only align proprioception with vision, but also predict changes in these variables as a consequence of a planned and ongoing motor commands.

Now consider what might happen if the reader could not see the notepad in the first place. How could the motor system compute the location of an unseen target in visual coordinates? The answer is that the notepad had fallen in the reader's field of view in the past, perhaps even on the fovea, and the motor system retained that information—in memory—in the form of the notepad's location in fixation-centered coordinates, as illustrated in Figure 4C. (Note that the target in Figure 4C has fixation-centered—but not retinotopic—coordinates.) The motor system stores and updates the location of potential targets relative to the fixation point as eye, head, and body movements reorient gaze (Gaffan and Hornak, 1997), and this information remains valid even when the target lies outside the visual field. Regions of cortex posterior to the posterior parietal cortex need to interact with frontal areas for such remapping from memory to occur (Gaffan and Hornak, 1997).

This updating mechanism also subserves hand–eye coordination. Ariff, Donchin, Nanayakkara, and Shadmehr (2002) have shown that as the hand moves during a reach, the motor system updates its estimate $\hat{x}_{ee}$ based on efference copy. For a saccade at time *t*, the new fixation point best correlates with hand location 150 ms later (Figure 5). This result suggests that the motor system updates $\hat{x}_{ee}$ as a reaching movement progresses. Because the estimate of hand location leads the actual hand location, the updating mechanism probably relies on efference copy.

If the motor system plans to move the eyes or the arm, it can update estimates of target- and end effector locations through an IM of the mechanical dynamics of the arm. This idea is illustrated in Figure 6. Such IMs are often called *forward models*. They describe how a physical object, such as an arm, should change state *(e.g.,* location and velocity), given that it was acted upon by a force (Jordan and Rumelhart, 1992; Miall, Weir, Wolpert, and Stein, 1993). The concept of forward models helps explain

the oculomotor behavior illustrated in Figure 5. As the motor system sends commands u_{ee} to the arm muscles to produce force, it also sends a copy of these commands $\hat{u}_{ee}$ to the forward model that estimates hand location $\hat{x}_{ee}$, presumably in the posterior parietal cortex. This IM also receives proprioceptive information $\hat{\theta}$ from the arm, but it arrives later. The "lagging" proprioceptive information $\hat{\theta}(t-\Delta)$ tells the network the arm's configuration a little while ago. The efference copy $\hat{u}_{ee}(t)$ tells it the commands that are about to act on the arm. Given the lagging proprioceptive information $\hat{\theta}(t-\Delta)$ and the current efference copy $\hat{u}_{ee}(t)$, the forward model of arm dynamics predicts end-effector location at some future time $\hat{x}_{ee}(t+\Delta)$. As the movement unfolds, the accuracy of that prediction can be detected, and the forward model adjusted as necessary to produce accurate predictions in the future.

Learning the dynamics map

ADAPTING TO NOVEL FORCE FIELDS

The primate arm has inertial dynamics that result in a complex relationship between motion and forces. In order to reliably make even the simplest movements, the motor system must *predict* the specific force requirements of a movement in generating the motor commands. We can think of this prediction as an alignment between a desired set of joint rotations and forces, *i.e.,* $\Delta\hat{\theta} \xleftrightarrow{\hat{\theta}} \hat{f}$, depicted as network 5 in Figure 2.

The accuracy and adaptability of force prediction is particularly important for reaching because holding different objects can dramatically change mechanical dynamics of the arm, and the motor system must accommodate this variability. In experiments aimed at studying this kind of adaptation, participants reach to a target while holding the handle of a robot, which imposes forces of various kinds (Shadmehr and Mussa-Ivaldi, 1994). In a typical experiment, when the robot's motors are off (called the *null-field condition*), participants make straight movements (Figure 7A). When the robot applies a force field that depended on the velocity of the hand (Figure 7B), these forces perturb the movement trajectory (Figure 7C). With practice, however, participants learn to make smooth and nearly straight movements despite the force field. *Catch trials*—relatively rare, intermixed trials in which the robot does not impose the force field—revealed the motor system's ability to predict the initially novel forces and modify motor commands accordingly. Early in training with the novel forces, the participants make straight movements in catch trials. With further experience in the field, participants made straight movements in the force field, but their movements in catch trials resemble a negative image of the early, perturbed movements

(Figure 7D). Catch trials demonstrate aftereffects of adaptation, the results of adapting the dynamics map.

The expression $\Delta\hat{\theta} \overset{\hat{\theta}}{\longleftrightarrow} \hat{f}$ assumes that internal models of dynamics are maps that align a representation of limb state with forces. Conditt, Gandolfo, and Mussa-Ivaldi (1997) considered the merits of an alternate idea, according to which something analogous to a tape recorder might store the forces that were sensed in the previous movements. Movement direction and time provide the inputs to this imaginary tape-recorder system, which produces force as its output. Such a system would also adapt reaching movements to the force field, without mapping joint displacement to force through an IM. To test this alternative, participants practiced reaching straight to a small number of targets while the novel force field was applied and later tried to draw a circle in the same field. If the motor system learned something like a tape recording of the forces encountered in reaching to each target, then there should be little generalization to much longer, circular movements. However, Conditt et al. observed good performance for circular movements in the force field and, importantly, the subjects showed aftereffects when the robot ceased imposing the forces. This finding indicates that the neural system did not predict forces explicitly as a function of time. Rather, it learned to associate the states of the arm—primarily its location and velocity—with forces. The order in which those states were visited did not matter. What was important was arm's velocity at locations traversed by the hand during reaching. These experiments indicate that with practice, participants adapted an IM of dynamics.

Consolidation of kinematics and dynamics maps

Behavioral measurements suggest that the IM of dynamics changed not only during the training session, but also in the hours that followed completion of training (Shadmehr and Brashers-Krug, 1997). The IM appeared to gradually change from an initially fragile state to a more resistant one during a period of ~5 hours. Similarly, in a task that required participants to adapt to the dynamics of an inertial object, Krakauer et al. (2000) reported that the IM for one object could be disrupted if participants immediately practices movements with a different object. Finally, disruptive transcranial magnetic stimulation (TMS) of primary motor cortex (M1) immediately after participant's practiced a thumb-flexion movement resulted in marked retention deficits, whereas stimulation 5 hours after practice did not (Muellbacher et al., 2002). Therefore, the passage of time alters the networks underlying the IMs in a way that consolidates their attractors.

Generalization of motor learning

In order to consider why adaptation to kinematic or dynamic perturbations produces a specific pattern of generalization, we need to go beyond a description of the variables that IMs align, to consider how the motor system might encode these variables. A population code provides one approach. Georgopoulos, Kalaska, Caminiti, and Massey (1982) first suggested one kind of population code, called the population vector, and although alternatives have been suggested subsequently, their ideas serve the present purposes. According to their idea, each cell has a preferred direction (PD), which can be represented as a vector of unit length $\mathbf{w}_i$. For movement direction α, each cell i discharges at a rate r_i, which can be decomposed into two terms: average activity $g_i(\alpha)$ for a variety of movement directions and noise:

$$r_i = g_i(\alpha) + n_i$$

Experiments show that the M1 tuning curves approximate gaussian or cosine-like functions with half-widths at half-maximum values of ~56^o (Amirikian and Georgopoulos, 2000). Experiments on neurons in visual cortex suggest that the noise term distributes normally with a variance proportional to the mean value of the tuning function (Tolhurst and Thompson, 1982). If cells did not have noise, a winner-take-all scheme might work well: to estimate which movement direction would move the end effector to the target, the motor system could simply determine that cell j discharged most during some movement and estimate the appropriate movement direction $\hat{\alpha}$ to be the PD of that cell: $\hat{\alpha} = \mathbf{w}_j$. However, because cells are noisy, that estimate would have a large variance from trial to trial. A population code, employing the law of large numbers, avoids this problem because each cell's discharge is weighted by its PD vector: each cell in the population contributes to the network's output in its PD and does so in proportion to its activity for a given movement direction on a given trial. The sum of these vectors should vary less that a winner-take-all system in producing an estimate of movement direction:

$$\hat{\alpha} = \sum_i \mathbf{w}_i r_i = \sum_i (\mathbf{w}_i g_i(\alpha) + \mathbf{w}_i n_i) \qquad (1)$$

The success of this kind of population coding depends on computing with neurons that broadly encode the input variable (Seung and Sompolinsky, 1993).

The example of population coding described in Eq. 1 provides an instance of "identity mapping", *i.e.,* a mapping where the output is an estimate of the input variable. Network 2 in our model provides another example. However, population codes can also map one input variable into another variable (Poggio, 1990; Pouget, Dayan, and Zemel, 2000):

$$\hat{y} = \sum_i (\mathbf{w}_i g_i(\alpha) + \mathbf{w}_i n_i) \qquad (2)$$

For the example of population coding described in Eq. 2, the tuning curves of the neurons that participate in this computation become *basis functions* used to approximate output *y*. Basis functions are a set of functions that, when linearly combined, can approximate almost any linear or nonlinear function (Pouget and Sejnowski, 1997). Thus, population coding can be used to compute identity maps, as well as for the more general problem of computing linear and nonlinear functions. Note, however, that whereas in the population code for estimating movement direction (Eq. 1), the weights were fixed vectors in a cell's PD, for learning alignment maps (Eq. 2), the weight vectors change and have no specific relationship with the tuning function $g_i(\alpha)$.

Let us now return to the problem of how the motor system might compute an IM of dynamics, $\Delta\hat{\theta} \xleftrightarrow{\hat{\theta}} \hat{f}$. This mapping aligns a state of the arm (*i.e.,* the desired displacement of the arm at a given position) with force **f**. Assume (1) that the networks use a population code, (2) that each neuron has a tuning curve g_i that describes the average discharge of that cell as a function of hand location and velocity, and (3) that each cell also has a preferred force vector $\mathbf{w}_i$. The population vector for force can be estimated, as follows:

$$\hat{\mathbf{f}} = \sum_i \mathbf{w}_i g_i\left(\theta, \Delta\theta\right) + \mathbf{w}_i n_i$$

We now have a framework for relating tuning properties with behavioral generalization during adaptation to force fields. Consider the following experiment: participants experience force $\mathbf{f}_1$ as they move their arm in certain locations with certain velocities, which we call state $\mathbf{x}_1$. The error that they experience in a movement changes weights **w**. Assuming Hebbian learning rules, the largest weight changes occur for those neurons that are most active when the arm was in or near state $\mathbf{x}_1$. Later, the participant makes reaching movements in other locations and/or with different velocities (state $\mathbf{x}_2$). If performance in state $\mathbf{x}_2$ after training differs from that in the naïve condition, then the basis function g_i must be broad enough to be active in both $\mathbf{x}_1$ and $\mathbf{x}_2$. Therefore, if the IM is represented via a population code, the generalization function should correspond to the shape of the tuning curves—the basis functions—of the neural elements implementing its computation.

This prediction depends, of course, on the assumptions stated above, which treat neurons in the motor system as spatial analyzers. Nevertheless, the theory predicts that if the neurons that subserve a given kind of motor learning have a given tuning property, then those properties affect the way in which motor learning generalizes.

GENERALIZING LOCATION MAPS

As described above (see

Figure 3), prism adaptation alters both the location and the displacement maps. To study how each map is constructed, and how adaptation of each mapping generalizes, it is important to devise experiments that require adaptation of one map but not the other.

In an experiment that isolated the location map (network 1), participants could view their hand only in one restricted location (Vetter, Goodbody, and Wolpert, 1999). At that location, the visual information was altered so that the visual information regarding hand location did not match proprioception, and participants had to learn a new alignment $\left(\hat{\theta}+\varepsilon\right)\leftrightarrow\hat{x}_{ee}$. Adaptation of the location map at this single target location had global consequences, *i.e.,* it affected movements to distant targets. Thus, the map $\hat{\theta}\leftrightarrow\hat{x}_{ee}$ must be computed with spatial analyzers that broadly encode joint-angular coordinates of the limb. In accord with this pattern of generalization, many neurons in the motor system encode static limb position with very broad, often linear functions (Helms Tillery, Soechting, and Ebner, 1996; Georgopoulos, Caminiti, and Kalaska, 1984; Bosco, Rankin, and Poppele, 1996).

Generalizing Displacement Maps

In order to isolate the displacement map, a different experimental design is needed. The goal is to leave the relationship between proprioception and vision for locations minimally changed, but dramatically change it for displacements. For normally viewed reaching movements, this goal is impossible to achieve, although it might be approximated for small differences in location. For cursors on a video monitor, however, this goal can be achieved easily: there should be no expectation that a cursor on a video monitor should match the proprioceptively sensed location of the hand. Cunningham (1989) pioneered this motor-learning paradigm, often called "rotation experiments." These experiments vary the relationship between joint-angle changes and end-effector displacements. For example, in one condition movements of the participant's hand to the left cause a movement of a cursor—the end effector—to the left, but in a "rotated" condition, same hand movements cause the cursor to move downward, a –90° rotation. To move the cursor to a target, the motor system must learn to map the desired cursor displacement to a new set of joint rotations: $x_{dv}\overset{\hat{\theta}}{\longleftrightarrow}\left(\Delta\hat{\theta}+\delta\right)$.

Rotation experiments study adaptation of displacement maps (Krakauer, Pine, Ghilardi, and Ghez, 2000). Krakauer et al. (2000) observed that adaptation had only a local effect on reaching movements; movements trained in one location generalize only to neighboring directions, with little effect at movement angles, in polar coordinates, that differed by more than 45° from the "trained" movement direction. This finding implies that the displacement map is computed with elements that have more selective tuning functions than those involved in computing the location map. The angular distance over which adaptation generalized is consistent with spatial analyzers having tuning functions similar to those

observed in M1 and the dorsal premotor cortex (PMd) (Caminiti, Johnson, Burnod, Galli, and Ferraina, 1990; Kalaska, Crammond, Cohen, Prud'homme, and Hyde, 1992), among other cortical and subcortical structures, such as the cerebellum (Johnson and Ebner, 2000; Fortier, Kalaska, and Smith, 1989) and basal ganglia (Turner and Anderson, 1997).

GENERALIZING DYNAMICS MAPS

Shadmehr and Moussavi (2000) observed that adaptation to forces in one arm configuration generalized to another, very different arm configuration. Note that very different arm configurations imply that the end effector, the hand, is in a very distant part of the workspace. The finding of Shadmehr and Moussavi means that the basis functions that compute $\Delta\hat{\theta} \xleftrightarrow{\hat{\theta}} \hat{f}$ must encode limb configuration quite broadly. As mentioned above, neurons in different parts of the motor system can be modulated globally and often linearly as a function of end-effector location (Georgopoulos et al., 1984; Bosco et al., 1996; Helms Tillery et al., 1996; Sergio and Kalaska, 2003). Activity with that property occurs in M1, area 5d, and in cells giving rise to the dorsal spinocerebellar tract. These findings support the idea that cells with global, planar tuning functions play an important role in computing the dynamics map. Using this approach, generalization patterns have been used to make the following additional inferences about the nature of encoding in the internal model of dynamics:

- The basis functions encode hand *velocity* with spatial analyzers that have a PD and but may be bimodally tuned (Donchin and Shadmehr, 2002)
- The PDs of the basis functions rotate with the shoulder angle (Shadmehr and Moussavi, 2000).
- Basis functions have weak, but distinct, sensitivity to movements of the ipsilateral arm, and the PD of the basis functions remain arm-invariant if the workspace is near the midline (Hemminger, Donchin, Ariff, Young, and Shadmehr, 2001).

With the exception of bimodal tuning, neurons with all of these properties have been reported for M1, basal ganglia, and cerebellum (Georgopoulos et al., 1984; Caminiti, Johnson, Galli, Ferranina, and Burnod, 1991; Turner and Anderson, 1997; Johnson and Ebner, 2000). The invariance of the preferred direction with respect to movements of the contralateral and ipsilateral arms has been reported recently for M1 (Steinberg et al., 2002) and PMd (Cisek, Crammond, and Kalaska, 2003). Bimodal tuning in arm velocity space has been observed in the cerebellum (Coltz, Johnson, and Ebner, 1999), but not in M1 for the same task (Johnson and Ebner, 2000). We recognize the indirect nature of this argument, but these correlations remain intriguing and should lead to further testable predictions.

NEURAL BASIS OF ADAPTING KINEMATICS

Adaptation of maps that align kinematic variables (networks 1 and 4 in

Figure 2) appears to depend on three brain regions: the posterior parietal cortex, the premotor cortex, and the cerebellum. Patients (Weiner, Hallett, and Funkenstein, 1983; Martin, Keating, Goodkin, Bastian, and Thach, 1996a) and monkeys (Baizer, Kralj-Hans, and Glickstein, 1999) with cerebellar damage have deficits in adapting to prisms. One study employing a rotation experiment showed a deficits in adapting the displacement map after inactivating the dentate nucleus of the cerebellum (Robertson and Miall, 1999). Clower et al. (1996) presented neuroimaging support of a role of posterior parietal cortex in prism adaptation. And Kurata and Hoshi (1999) showed that temporary inactivation of PMv causes a deficit in prism adaptation in monkeys.

The most extensive analysis of neuronal activity during the adaptation of displacement maps has been for "rotation" experiments (Wise, Moody, Blomstrom, and Mitz, 1998; Moody and Wise, 2001), although other transforms have also been used. As a population, cells in PMd, the supplementary motor area (SMA), and M1 all showed dramatic changes in their properties during adaptation of displacement maps. These changes took the form of changes in the cells PD, which were often very large, and changes in both the depth of tuning and the width of tuning. Approximately half of the sample of neurons in these areas showed significant changes in activity during adaptation and, as a population, this activity change appeared to lag the adaptation as measured behaviorally. This finding may be relevant to the time-course of consolidation noted above, but remains poorly understood.

NEURAL BASIS OF ADAPTING DYNAMICS

Adaptation of the dynamics map also depends on cerebellar function (Smith, 2001). Patients with cerebellar disease showed a marked inability to adapted to the forces imposed by the robot and showed little of no aftereffect. M1 probably also contributes to adapting the dynamics map, although the evidence for this idea is much less direct than for cerebellum. A collection of muscles can substitute for the force variable as network 5's output (

Figure 2). Thoroughman and Shadmehr (1999) extended the

Figure 2 model in this way and noted that—for a particular class of force fields—adaptation produced a rotation in the preferred direction (PD) of arm muscles. M1 cells and muscles in monkeys show a median clockwise PD shift of comparable amounts as they adapt to the same force field (Li, Padoa-Schioppa, and Bizzi, 2001). In addition, Bizzi and his colleagues found that, whereas the EMG patterns returned to

baseline conditions once the field was turned off (*i.e.*, during washout trials), many cells in M1 retained their new PD. Other cells showed changes in PD specifically during the washout trials. As a population, these changes in PD balanced each other so that the population vector remained a good description of end effector's movement direction. Further analysis revealed similar phenomena in PMd and SMA, with an additional finding regarding SMA (Padoa-Schioppa, Li, and Bizzi, 2002). During an instructed-delay period, cells in SMA showed an increasing reflection of the forces needed to move the limb to the target. Thus, Padoa-Schioppa et al. concluded that SMA plays a role in the kinematics-to-dynamics transform $\Delta\hat{\theta} \xleftarrow{\hat{\theta}} \hat{f}$.

Summary

Reaching relies on computations that transform proprioceptive and exteroceptive information—in fixation-centered coordinates—into motor commands, and all of these mappings adapt. Altering vision with prisms, for example, changes the alignment between proprioception and hand location (mapping 1) as well as that between the difference vector and joint rotations (mapping 4). Altering the weight of the arm or imposing forces on it during movement changes the mapping of joint rotations onto force commands (mapping 5). With repeated adaptation, often consuming many weeks and hundreds of movements, new IMs form that can be recalled with contextual cues. For visually guided reaching in primates, motor learning begins with the adaptation of existing IMs and ends in formation of new ones. The motor system has acquired a new skill.

ACKNOWLEDGEMENTS We thank Dr. Paul Cisek for comments on an earlier version of this paper.

AMIRIKIAN, B., and A. P. GEORGOPOULOS. 2000. Directional tuning profiles of motor cortical cells. *Neurosci. Res., 36:* 73-79.

ANDERSEN, R. A., R. M. BRACEWELL, S. BARASH, J. W. GNADT, and L. FOGASSI. 1990. Eye position effects on visual, memory, and saccade-related activity in areas LIP and 7a of macaque. *J. Neurosci., 10:* 1176-1196.

ANDERSEN, R. A., and C. A. BUNEO. 2002. Intentional maps in posterior parietal cortex. *Annu. Rev. Neurosci., 25:* 189-220.

ARIFF, G., O. DONCHIN, T. NANAYAKKARA, and R. SHADMEHR. 2002. A real-time state predictor in motor control: Study of saccadic eye movements during unseen reaching movements. *J. Neurosci., 22:* 7721-7729.

BAIZER, J. S., I. KRALJ-HANS, and M. GLICKSTEIN. 1999. Cerebellar lesions and prism adaptation in macaque monkeys. *J. Neurophysiol., 81:* 1960-1965.

BOSCO, G., A. RANKIN, and R. E. POPPELE. 1996. Representation of passive hindlimb postures in cat spinocerebellar activity. *J. Neurophysiol., 76:* 715-726.

BREMMER, F., C. DISTLER, and K. P. HOFFMANN. 1997. Eye position effects in monkey cortex. II. Pursuit- and fixation-related activity in posterior parietal areas LIP and 7A. *J. Neurophysiol., 77:* 962-977.

BULLOCK, D., and S. GROSSBERG. 1988. The VITE model: A neural command circuit for generating arm and articulator trajectories. In *Dynamic Patterns in Complex Systems*, J. A. S. Kelso, A. J. Mandell, and M. F. Shlesinger, eds. Singapore: World Scientific Publishers, (pp. 305-326).

BURNOD, Y., P. BARADUC, A. BATTAGLIA-MAYER, E. GUIGON, E. KOECHLIN, S. FERRAINA, F. LACQUANITI, and R. CAMINITI. 1999. Parieto-frontal coding of reaching: an integrated framework. *Exp Brain Res, 129:* 325-346.

CAMINITI, R., P. B. JOHNSON, Y. BURNOD, C. GALLI, and S. FERRAINA. 1990. Shift of preferred directions of premotor cortical cells with arm movements performed across the workspace. *Exp. Brain Res., 83:* 228-232.

CAMINITI, R., P. B. JOHNSON, C. GALLI, S. FERRANINA, and Y. BURNOD. 1991. Making arm movements within different parts of space: The premotor and motor cortical representation of a coordinate system for reaching to visual targets. *J. Neurosci., 11:* 1182-1197.

CISEK, P., D. J. CRAMMOND, and J. F. KALASKA. 2003. Neural activity in primary motor and dorsal premotor cortex in reaching tasks with the contralateral versus ipsilateral arm. *J. Neurophysiol., 89:* 922-942.

CISEK, P., S. GROSSBERG, and D. BULLOCK. 1998. A cortico-spinal model of reaching and proprioception under multiple task constraints. *J. Cogn. Neurosci., 10:* 425-444.

CLOWER, D. M., J. M. HOFFMAN, J. R. VOTAW, T. L. FABER, R. P. WOODS, and G. E. ALEXANDER. 1996. Role of posterior parietal cortex in the recalibration of visually guided reaching. *Nature, 383:* 618-621.

COLTZ, J. D., M. T. V. JOHNSON, and T. J. EBNER. 1999. Cerebellar Purkinje cell simple spike discharge encodes movement velocity in primates during visuomotor arm tracking. *J. Neurosci., 19:* 1782-1803.

CONDITT, M. A., F. GANDOLFO, and F. A. MUSSA-IVALDI. 1997. The motor system does not learn the dynamics of the arm by rote memorization of past experience. *J. Neurophysiol., 78:* 554-560.

CUNNINGHAM, H. A. 1989. Aiming error under transformed spatial mappings suggests a structure for visual-motor maps. *J. Exp. Psychol., 15:* 493-506.

DENEVE, S., P. E. LATHAM, and A. POUGET. 2001. Efficient computation and cue integration with noisy population codes. *Nat. Neurosci., 4:* 826-831.

DESMURGET, M., C. M. EPSTEIN, R. S. TURNER, C. PRABLANC, G. E. ALEXANDER, and S. T. GRAFTON. 1999. Role of the posterior parietal cortex in updating reaching movements to a visual target. *Nat. Neurosci., 2:* 563-567.

DESMURGET, M., D. PELISSON, Y. ROSSETTI, and C. PRABLANC. 1998. From eye to hand: planning goal-directed movements. *Neurosci. Biobehav. Rev., 22:* 761-788.

DONCHIN, O., and R. SHADMEHR. 2002. Linking motor learning to function approximation: Learning in an unlearnable force field. *Adv. Neural Inform. Proc. Sys. 14:*197-203.

DUHAMEL, J.-D., C. L. COLBY, and M. E. GOLDBERG. 1992. The updating of the representation of visual space in parietal cortex by intended eye movements. *Science, 255:* 90-92.

FORTIER, P. A., J. F. KALASKA, and A. M. SMITH. 1989. Cerebellar neuronal activity related to whole-arm reaching movements in the monkey. *J. Neurophysiol., 62:* 198-211.

GAFFAN, D., and J. HORNAK. 1997. Visual neglect in the monkey. Representation and disconnection. *Brain, 120:* 1647-1657.

GEORGOPOULOS, A. P., R. CAMINITI, and J. F. KALASKA. 1984. Static spatial effects in motor cortex and area 5: quantitative relations in a two-dimensional space. *Exp. Brain Res., 54:* 446-454.

GEORGOPOULOS, A. P., J. F. KALASKA, R. CAMINITI, and J. T. MASSEY. 1982. On the relations between the direction of two-dimensional arm movements and cell discharge in primate motor cortex. *J. Neurosci., 2:* 1527-1537.

GREA, H., L. PISELLA, Y. ROSSETTI, M. DESMURGET, C. TILIKETE, S. GRAFTON, C. PRABLANC, and A. VIGHETTO. 2002. A lesion of the posterior parietal cortex disrupts on-line adjustments during aiming movements. *Neuropsychologia, 40:* 2471-2480.

HALLETT, M., A. PASCUAL-LEONE, and H. TOPKA. 1996. Adaptation and skill learning: Evidence for different neural substrates. In *The acquisition of motor behavior in vertebrates*, J. R. Bloedel, T. J. Ebner, and S. P. Wise, eds. Cambridge: MIT Press, (pp. 289-301).

HARRIS, C. S. 1965. Perceptual adaptation to inverted, reversed, and displaced vision. *Psychol. Rev., 72:* 419-444.

HELMS TILLERY, S. I., J. F. SOECHTING, and T. J. EBNER. 1996. Somatosensory cortical activity in relation to arm posture: nonuniform spatial tuning. *J. Neurophysiol., 75:* 2423-2438.

HEMMINGER, S. E., O. DONCHIN, G. D. ARIFF, E. D. YOUNG, and R. SHADMEHR. 2001. Intermanual generalization of arm dynamics in extrinsic coordinates. *Soc. Neurosci. Abs., 302.1*

JOHNSON, M. T. V., and T. J. EBNER. 2000. Processing of multiple kinematic signals in the cerebellum and motor cortices. *Brain Res. Rev., 33:* 155-168.

JORDAN, M. I., and D. E. RUMELHART. 1992. Forward models: supervised learning with a distal teacher. *Cogn. Sci., 16:* 307-354.

KALASKA, J. F., D. J. CRAMMOND, D. A. D. COHEN, M. PRUD'HOMME, and M. L. HYDE. 1992. Comparison of cell discharge in motor, premotor, and parietal cortex during reaching. In *Control of Arm Movement in Space: Neurophysiological and Computational Approaches*, R. Caminiti and P. Johnson, eds. Berlin: Springer-Verlag, (pp. 129-146).

KRAKAUER, J. W., Z. M. PINE, M. F. GHILARDI, and C. GHEZ. 2000. Learning of visuomotor transformations for vectorial planning of reaching trajectories. *J. Neurosci., 20:* 8916-8924.

KURATA, K., and E. HOSHI. 1999. Reacquisition deficits in prism adaptation after muscimol microinjection into the ventral premotor cortex of monkeys. *J. Neurophysiol., 81:* 1927-1938.

LI, C. S., C. PADOA-SCHIOPPA, and E. BIZZI. 2001. Neuronal correlates of motor performance and motor learning in the primary motor cortex of monkeys adapting to an external force field. *Neuron, 30:* 593-607.

MARTIN, T. A., J. G. KEATING, H. P. GOODKIN, A. J. BASTIAN, and W. T. THACH. 1996a. Throwing while looking through prisms. I. Focal olivocerebellar lesions impair adaptation. *Brain, 119:* 1183-1198.

MARTIN, T. A., J. G. KEATING, H. P. GOODKIN, A. J. BASTIAN, and W. T. THACH. 1996b. Throwing while looking through prisms. II. Specificity and storage of multiple gaze-throw calibrations. *Brain, 119:* 1199-1211.

MIALL, R. C., D. J. WEIR, D. M. WOLPERT, and J. F. STEIN. 1993. Is the cerebellum a Smith predictor? *J. Motor Behav., 25:* 203-216.

MOODY, S. L., and S. P. WISE. 2001. Connectionist contributions to population coding in the motor cortex. *Prog. Brain Res., 130:* 245-266.

MUELLBACHER, W., U. ZIEMANN, J. WISSEL, N. DANG, M. KOFLER, S. FACCHINI, B. BOROOJERDI, W. POEWE, and M. HALLETT. 2002. Early consolidation in human primary motor cortex. *Nature, 415:* 640-644.

PADOA-SCHIOPPA, C., C. S. LI, and E. BIZZI. 2002. Neuronal correlates of kinematics-to-dynamics transformation in the supplementary motor area. *Neuron, 36:* 751-765.

POGGIO, T. 1990. A theory of how the brain might work. *Cold Spring Harbor Symp. Quant. Biol., 55:* 899-910.

POUGET, A., P. DAYAN, and R. ZEMEL. 2000. Information processing with population codes. *Nat. Rev. Neurosci., 1:* 125-132.

POUGET, A., and T. J. SEJNOWSKI. 1997. Spatial transformations in the parietal cortex using basis functions. *J. Cog. Neurosci., 9:* 222-237.

ROBERTSON, E. M., and R. C. MIALL. 1999. Visuomotor adaptation during inactivation of the dentate nucleus. *NeuroReport, 10:* 1029-1034.

SALINAS, E., and L. F. ABBOTT. 2001. Coordinate transformations in the visual system: how to generate gain fields and what to compute with them. In *Progress in Brain Research*, M. A. L. Nicolelis, ed. Elsevier, (pp. 175-190).

SEKIYAMA, K., S. MIYAUCHI, T. IMARUOKA, H. EGUSA, and T. TASHIRO. 2000. Body image as a visuomotor transformation device revealed in adaptation to reversed vision. *Nature, 407:* 374-377.

SERGIO, L. E., and J. F. KALASKA. 2003. Systematic changes in motor cortex cell activity with arm posture during directional isometric force generation. *J. Neurophysiol., 89:* 212-228.

SEUNG, H. S., and H. SOMPOLINSKY. 1993. Simple models for reading neuronal population codes. *Proc. Natl. Acad. Sci. U.S.A, 90:* 10749-10753.

SHADMEHR, R., and T. BRASHERS-KRUG. 1997. Functional stages in the formation of human long-term motor memory. *J. Neurosci., 17:* 409-419.

SHADMEHR, R., and Z. M. K. MOUSSAVI. 2000. Spatial generalization from learning dynamics of reaching movements. *J. Neurosci., 20:* 7807-7815.

SHADMEHR, R., and F. A. MUSSA-IVALDI. 1994. Adaptive representation of dynamics during learning of a motor task. *J. Neurosci., 14:* 3208-3224.

SMITH, M. A. (2001) Error correction, the basal ganglia, and the cerebellum. Ph.D. Thesis, Johns Hopkins University.

SOMMER, M. A., and R. H. WURTZ. 2002. A pathway in primate brain for internal monitoring of movements. *Science, 296:* 1480-1482.

STEINBERG, O., O. DONCHIN, A. GRIBOVA, D. O. CARDOSA, H. BERGMAN, and E. VAADIA. 2002. Neuronal populations in primary motor cortex encode bimanual arm movements. *Eur. J. Neurosci., 15:* 1371-1380.

SUGITA, Y. 1996. Global plasticity in adult visual cortex following reversal of visual input. *Nature, 380:* 523-526.

THOROUGHMAN, K. A., and R. SHADMEHR. 1999. Electromyographic correlates of learning internal models of reaching movements. *J. Neurosci., 19:* 8573-8588.

TOLHURST, D. J., and I. D. THOMPSON. 1982. Organization of neurones preferring similar spatial frequencies in cat striate cortex. *Exp. Brain Res., 48:* 217-227.

TURNER, R. S., and M. E. ANDERSON. 1997. Pallidal discharge related to the kinematics of reaching movements in two dimensions. *J Neurophysiol, 77:* 1051-1074.

VETTER, P., S. J. GOODBODY, and D. M. WOLPERT. 1999. Evidence for an eye-centered spherical representation of the visuomotor map. *J. Neurophysiol., 81:* 935-939.

WEINER, M. J., M. HALLETT, and H. H. FUNKENSTEIN. 1983. Adaptation to lateral displacement of vision in patients with lesions of the central nervous system. *Neurology, 33:* 766-772.

WELCH, R. B., C. S. CHOE, and D. R. HEINRICH. 1974. Evidence for a three-component model of prism adaptation. *J. Exp. Psychol., 103:* 700-705.

WISE, S. P., S. L. MOODY, K. J. BLOMSTROM, and A. R. MITZ. 1998. Changes in motor cortical activity during visuomotor adaptation. *Exp. Brain Res., 121:* 285-299.

T

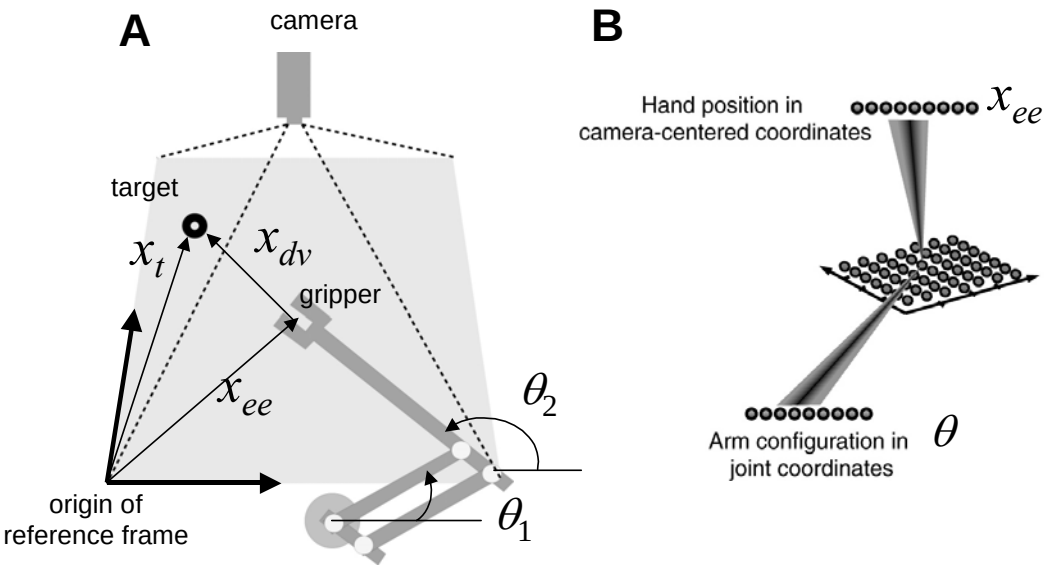

Figure 1. (A) A robotic arm that moves in two dimensions and a camera. The target *t* of the movement is the black ring. Gripper location and target locations are specified in camera-centered coordinates with vectors x_{ee} and x_t. The difference vector x_{dv}, also defined in camera-centered coordinates, is the distance and direction the gripper must move to reach the target. The joint-angle sensors on the robot measure joint angles θ_1 and θ_2. (B) Alignment of proprioception with vision. A recurrent neural network aligns estimate of end-effector location from the camera with the joint angle sensors with the camera. (B modified from Deneve et al. (2001))

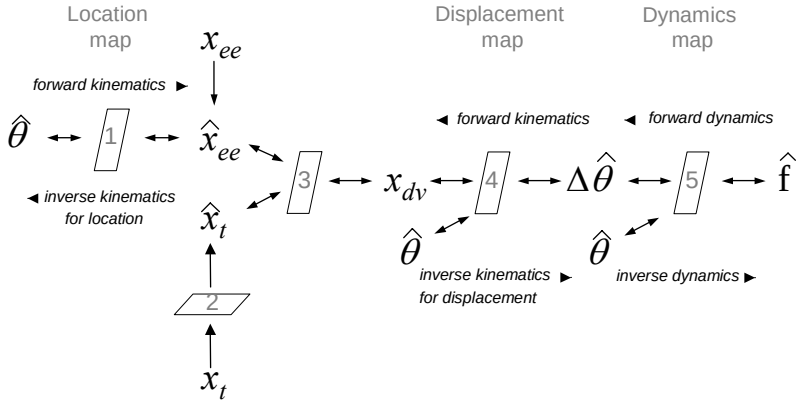

Figure 2. A schematic drawing of the computations involved in planning a reaching movement for the robotic arm illustrated in

Figure 1A. Each parallelogram represents a distributed neural network. Joint sensors provide a measure of arm configuration □ and a camera provides an estimate of hand and target location, x_{ee} and x_t, in camera-centered coordinates. A network with bidirectional connections associates joint and camera based estimate of hand location $\hat{\theta} \leftrightarrow \hat{x}_{ee}$. From the estimates of hand and target location, a difference vector x_{dv} is computed for the hand. This difference vector is then associated with a joint rotations needed to reach the target. Finally, these joint-angle changes need to be associated with the forces necessary to make the movement. Abbreviations: end effector, *ee*; difference vector, *dv*; target, *t*; joint angles, □ □ force, $\tilde{f}$

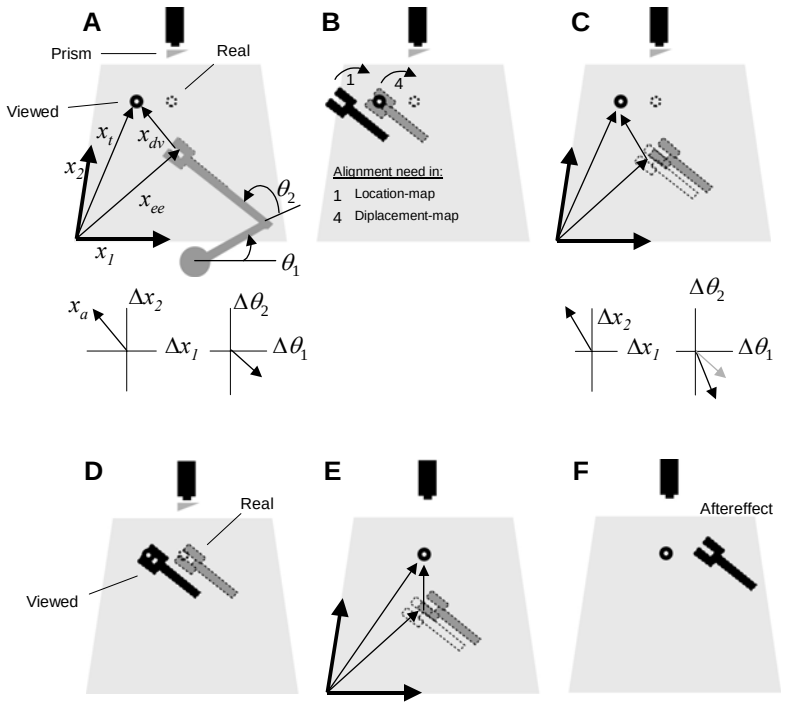

Figure 3. A prism that shifts the path of light to the left is inserted in front of the camera. (A) Before adaptation condition. Arm cannot be seen and gripper location is estimated from proprioception. Target location in real space is at the dotted circle but is sensed by the camera at the semi-filled circle. The subfigure below shows the desired hand displacement in camera-centered and joint-centered coordinates. (B) Result of the joint rotations. The camera sees the arm (black) miss the target to the left. Arm position in real space is drawn in gray. The curved arrows labeled 1 and 4 refer to adaptations of networks 1 and 4 in

Figure 2. (C) After adaptation, both the estimated gripper location and the difference vector in joint coordinates have changed. The joint-rotation vector prior to prism adaptation is shown as the gray arrow. Note that to reach the target after adaptation, θ_1 needs to increase less than before adaptation, whereas θ_2 needs to decrease more (more elbow extension). (D) Arm configuration at the end of the reaching movement after adaptation. (E) The prism is removed and the target is again presented. (F) The resulting reaching movement displays the aftereffect of adaptation.

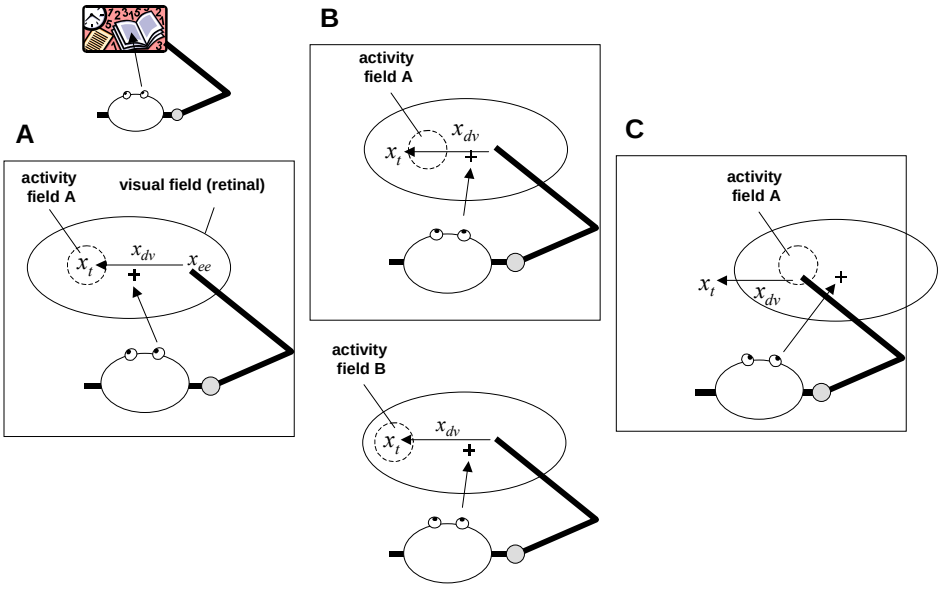

Figure 4. Need for updating target and end-effector locations due to reorientation of the fovea. (A) The participant fixates the plus sign; the ellipse indicates the limits of the entire visual field (not to scale). The circle (dashed line) shows the activity field (in this case, a receptive field) of an imaginary neuron. (B) Top: The participant's fixation point shifts to the right, so the visual field, as a whole, and the cell's activity field in retinocentric coordinates shifts by an equal amount. Bottom: The participant in the same situation as at the top, but a cell with a different activity field is illustrated. Note that the target x_t has shifted out of the top cell's activity field and into that of the second cell's. (C) Another eye movement in the same direction shifts the target out of the visual field entirely.

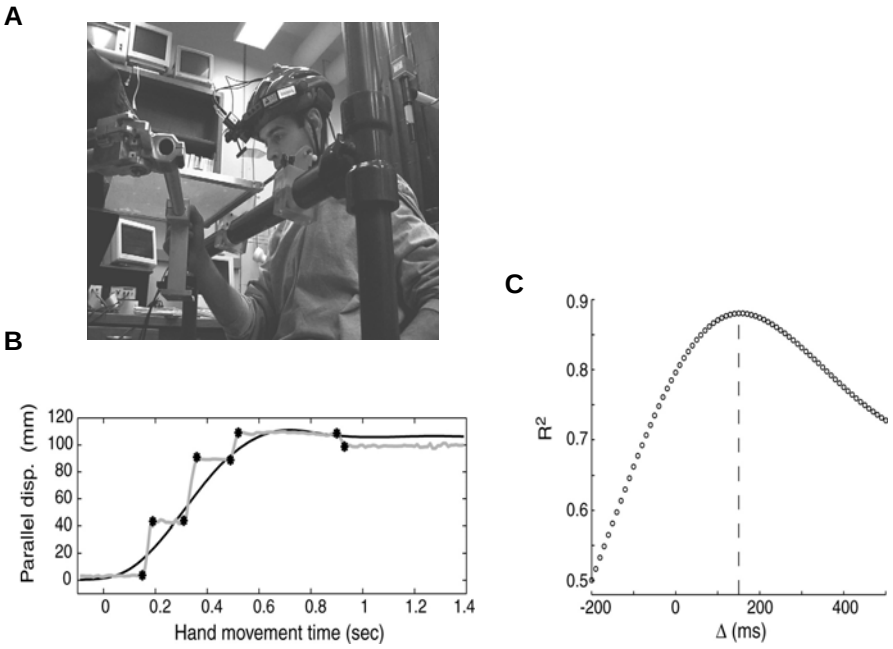

Figure 5. Estimating hand location during reaching movements. (A) Participants were asked to hold the handle of a robotic manipulandum while making reaching movements. They were instructed to look at their unseen hand as they reached to a remembered target location. The arm was not visible in the experiment but is shown uncovered here. (B) Hand location (black line) and eye orientation (gray line) are plotted for a typical movement. (C) Eye orientation at saccade endpoint correlates with end-effector location. Maximum correlation is at □= 150 ms, which means that participants fixate a location the hand will reach 150 ms later. (From Ariff, Donchin, Nanayakkara, and Shadmehr, 2002).

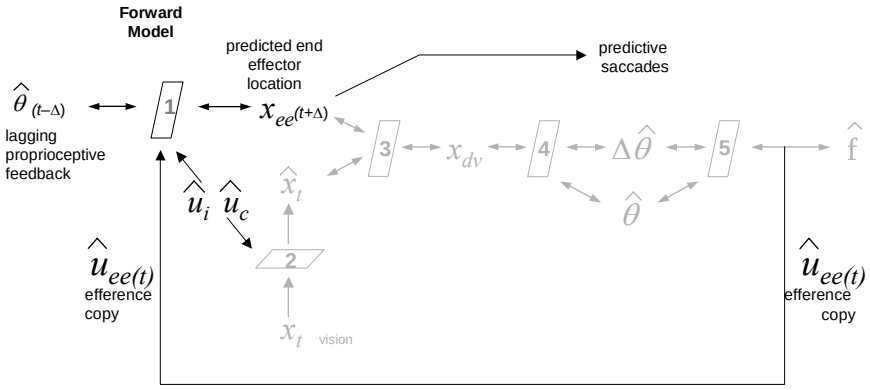

Figure 6. Predictive updating based on forward models and the influence of updating signals on the kinematic mappings depicted in Figure 2. Abbreviations as in Figure 2, plus: efference copy, *u*; eye, *i*; head (cranium), *c*.

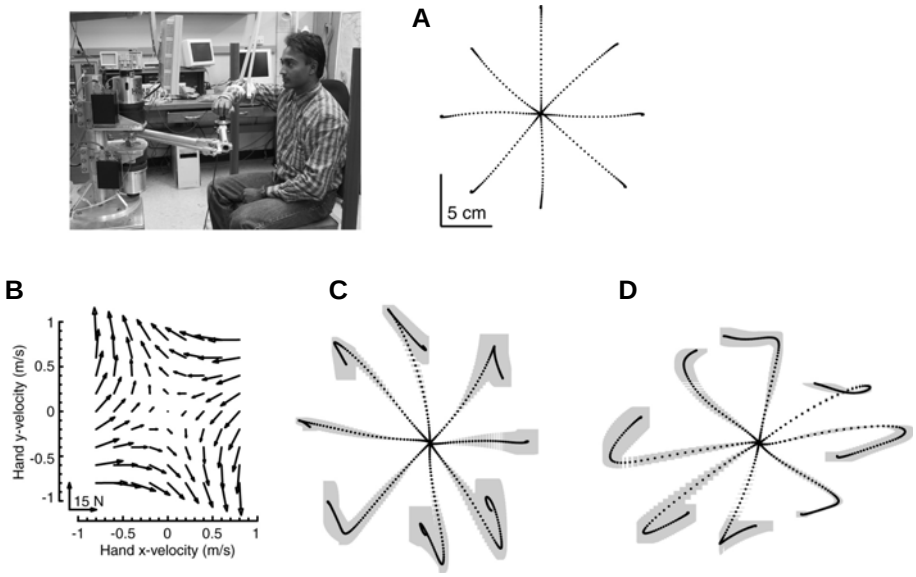

Figure 7. Experimental setup and typical data in a force field adaptation task. (A) Participants hold the handle of the robot and reach to a target. The plot shows hand trajectory (dots are 10 ms apart) for typical movements to eight targets. (B) The force field produced by the robot. Forces are plotted as a function of hand velocity. (C) Average hand trajectories (± S.D.) for movements during the initial trials in the force field. (D) Simulation results for movements in the force field. (E) Hand trajectories during catch trials. (F) Simulation results during catch trials. The controller in this simulation had fully adapted to the field and was expecting the field to be present in these movements. Abbreviation: S.D., standard deviation. (From Shadmehr and Mussa-Ivaldi 1994).

ENDNOTES

[1] The name *forward* kinematics reflects the fact that this computation corresponds to the causal direction of information flow: in this example, the gripper's location changes *because* joint angles change, so computing end-effector location from joint angles corresponds to a *forward* computation.

[2]The "hat" ^ over a symbol indicates a computed estimate rather than a transduced value.